European Radiology (2019) 29:1400–1407
https://doi.org/10.1007/s00330-018-5724-4

COMPUTED TOMOGRAPHY

Comparison of full-iodine conventional CT and half-iodine virtual monochromatic imaging: advantages and disadvantages

Haruto Sugawara[1,2] · Shigeru Suzuki[1] · Yoshiaki Katada[1] · Takuya Ishikawa[1] · Rika Fukui[1] · Yuzo Yamamoto[1] · Osamu Abe[2]

Received: 4 July 2018 / Revised: 5 August 2018 / Accepted: 16 August 2018 / Published online: 12 September 2018

Abstract

Purpose To compare image quality of abdominal arteries between full-iodine-dose conventional CT and half-iodine-dose virtual monochromatic imaging (VMI).

Materials and methods We retrospectively evaluated images of 21 patients (10 men, 11 women; mean age, 73.9 years) who underwent both full-iodine (600 mg/kg) conventional CT and half-iodine (300 mg/kg) VMI. For each patient, we measured and compared CT attenuation and the contrast-to-noise ratio (CNR) of the aorta, celiac artery, and superior mesenteric artery (SMA). We also compared CT dose index (CTDI). Two board-certified diagnostic radiologists evaluated visualisation of the main trunks and branches of the celiac artery and SMA in maximum-intensity-projection images. We evaluated spatial resolution of the two scans using an acrylic phantom.

Results The two scans demonstrated no significant difference in CT attenuation of the aorta, celiac artery, and SMA, but CNRs of the aorta and celiac artery were significantly higher in VMI ($p = 0.011$ and 0.030, respectively). CTDI was significantly higher in VMI ($p = 0.024$). There was no significant difference in visualisation of the main trunk of the celiac artery and SMA, but visualisation of the gastroduodenal artery, pancreatic arcade, branch of the SMA, marginal arteries, and vasa recta was significantly better in the conventional scan ($p < 0.001$). The calculated modular transfer function (MTF) suggested decreased spatial resolution of the half-iodine VMI.

Conclusion Large-vessel depiction and CNRs were comparable between full-iodine conventional CT and half-iodine VMI images, but VMI did not permit clear visualisation of small arteries and required a larger radiation dose.

Key Points

- *Reducing the dose of iodine contrast medium is essential for chronic kidney disease patients to prevent contrast-induced nephropathy.*
- *In virtual monochromatic images at low keV, contrast of relatively large vessels is maintained even with reduced iodine load, but visibility of small vessels is impaired with decreased spatial resolution.*
- *We should be aware about the advantages and disadvantages associated with virtual monochromatic imaging with reduced iodine dose.*

Keywords CT angiography · Iodine · Qualitative evaluation · Quantitative evaluation · Retrospective study

Abbreviations

AEC	Auto-exposure control
ASiR	Adaptive statistical iterative reconstruction
CIN	Contrast-induced nephropathy
CKD	Chronic kidney disease
CNR	Contrast-to-noise ratio
CT	Computed tomography
CTDI	Computed tomography dose index
DLP	Dose-length product
GDA	Gastroduodenal artery
HU	Hounsfield units
MIP	Maximum intensity projection
MTF	Modular transfer function
ROI	Region of interest
SD	Standard deviation

✉ Shigeru Suzuki
shig.suz@gmail.com

[1] Department of Radiology, Tokyo Women's Medical University Medical Center East, 2-1-10 Nishiogu, Arakawa-ku, Tokyo 116-8567, Japan

[2] Department of Radiology, Graduate School of Medicine, University of Tokyo, 7-3-1 Hongo, Bunkyo-ku, Tokyo 113-8655, Japan

SMA Superior mesenteric artery
VMI Virtual monochromatic imaging

Introduction

Computed tomography (CT) angiography is widely used to evaluate vessels throughout the body, and safe surgical or catheter intervention requires good understanding of the distribution of small arteries and anomalies in the branching of vessels around a lesion [1–3].

Visualisation of the small peripheral vessels in CT angiography necessitates the injection of a sufficient dose of iodine-based contrast medium. However, in patients with chronic kidney disease (CKD), the development of contrast-induced nephropathy (CIN) has been correlated with the excessive administration of contrast medium containing iodine, and minimal use of contrast has been recommended [4–6].

Recently, image reconstruction utilising virtual monochromatic imaging (VMI) in dual-energy CT has been adopted in an effort to reduce the amount of iodine-based contrast material needed in CT angiography. VMI allows an increase in intraluminal CT values at lower levels of energy, nearer those of the K-edge of iodine (33.2 keV) [7], which maintains vascular contrast even when the iodine dose is reduced. Indeed, past studies have reported comparable contrast-to-noise ratios (CNRs) in VMI-reconstructed images of CT angiography acquired with a reduced dose of iodine-based contrast medium and images of conventional CT angiography obtained using a full dose [8–10]. Nevertheless, the spatial resolution of the reconstruction method also affects the visualisation of small arteries [11], and we believe no study of CT angiography with VMI has examined spatial resolution and the visualisation of such peripheral arteries, though some researchers have focused on the CNR of relatively large vessels [8–10].

In emergent situation, the dose of iodine is not the main issue [12], and in preoperative situations, the need for better image quality, especially visualisation of small arteries, possibly takes priority to reduction of iodine dose to perform a safe procedure.

We therefore compared image quality between full-iodine-dose conventional CT and half-iodine-dose virtual monochromatic imaging in CT angiography to ascertain advantages and disadvantages of these two protocols.

Materials and methods

Calculation of the modulation transfer function

We calculated the modulation transfer function (MTF) using a phantom (Fig. 1) consisting of an elliptically shaped acrylic cylinder (diameter, about 30 × 20 cm; height, about 10 cm) with a columnar hole at its centre (diameter, about 4 cm; height, about 8 cm) that we filled with either a 20-fold dilution of iopamidol contrast medium (Oiparomin 300, Fuji Pharma Co., Ltd.) for conventional scanning or a 40-fold dilution for dual-energy scanning. For dual-energy scanning, we reconstructed virtual monochromatic images at 52 keV, setting scan parameters for the respective imaging systems to yield a similar CT dose index (CTDI; LightSpeed VCT, 120 kVp [GE Healthcare]; 34.99 mGy, Discovery CT750 HD 120 kVp [GE Healthcare]; 35.43 mGy; Discovery CT750 HD 52 keV; 33.96 mGy). We obtained the edge spread function at the edge of the iodine contrast material filling the cylinder in the acrylic phantom, differentiated the edge spread function to determine the line spread function, and applied fast Fourier transformation of the line spread function to obtain the MTF [13–15].

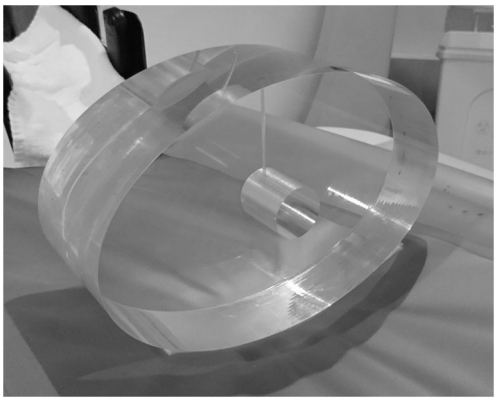

Fig. 1 Photograph of the acrylic phantom that we filled with contrast medium and used to calculate the modular transfer function (MTF) utilising a circular-edge technique

Patient population of the clinical study

Our institutional review board approved this retrospective single-centre study and waived the requirement for informed consent from participants.

We searched our CT database to identify consecutive patients who underwent VMI using the half-iodine-dose (300 mg/kg) protocol because of impaired kidney function (most recent estimated glomerular filtration rate less than 45 mL/min/1.73 m^2) between July 1 and September 30, 2016 and found 33 patients. We then further narrowed this group of 33 to 21 who also underwent conventional CT utilising the full-iodine-dose (600 mg/kg) protocol within the past 5 years (September 30, 2011 to September 30, 2016), and excluded the other 12. On average, the conventional scans were obtained 1.6 years before VMI acquisition. The study population comprised 21 patients (10 men, 11 women; mean age, 73.9 years; average body weight, 56.3 kg) who underwent CT screening for metastasis of colon cancer (n = 10), renal cancer (n = 6), cystic cancer (n = 3), uterine cancer (n = 1), and gastric cancer (n = 1). The scan ranges varied between the scan types and the individuals evaluated. The range was from the chest to

the pelvis in 19 of the 21 patients for half-iodine VMI and 12 of the 21 for full-iodine conventional CT and from the upper abdomen to the pelvis in the other 2 for half-iodine VMI and 9 for full-iodine conventional CT.

Scan protocol

Our conventional scan protocol called for the injection of 600 mg/kg of iodine contrast medium in 30 s, and the VMI protocol utilised half that dose, 300 mg/kg, injected in 30 s. The scan of the CT angiography was begun at 40 s after the start of contrast material injection.

For the full-dose protocol, parameters were: collimation, 64 × 0.625 mm; pitch, 1.375; gantry rotation, 0.4 second; scan field of view (FOV), 50 cm; and tube voltage, 120 kVp. Tube current was automatically changed with auto exposure control (AEC) with a noise index of 12. Nine of the 21 patients were scanned using the LightSpeed VCT system and 12 with the Discovery CT750 HD system.

For the half-iodine VMI protocol, parameters were: collimation, 64 × 0.625 mm; pitch, 1.375; scan FOV, 50 cm; tube voltage, fast kilovoltage switching between 80 and 140 kVp. Gantry rotation and tube current were determined depending on the patient's body size to achieve a noise index close to that of the conventional scan. All 21 patients were scanned with the Discovery CT750 HD system.

We employed a standard reconstruction kernel to reconstruct images of a section of 1.25-mm thickness and interval, and applied 40% adaptive statistical iterative reconstruction (ASiR) to reduce image noise. For VMI protocol, we reconstructed virtual monochromatic images at 52 keV.

Quantitative analysis of arteries

In axial images, circular regions of interest (ROIs) of 10-mm diameter were placed on the aorta (at the level between the orifice of the celiac artery and the SMA) and right psoas muscle, and circular ROIs of 2-mm diameter were placed on the main trunks of the celiac artery and SMA. CT attenuation was measured as the average CT values in these ROIs. Image noise was defined as the standard deviation (SD) of the CT values in the ROIs placed on the right psoas muscle. CNR was calculated as: $CNR = (\mu_A - \mu_B) / \rho$, in which μ_A is the signal intensity of the aorta, celiac artery, or SMA; μ_B is the signal intensity of the psoas major muscle, and ρ is the image noise.

We compared CTDI and dose-length product (DLP) between the VMI and conventional scans based on the dose report.

Subjective evaluation of proximal and peripheral arteries

We reconstructed coronal maximum intensity-projection (MIP) images (10-mm thickness, 1-mm interval) on the workstation (Advantage Workstation Version 4.6, GE Healthcare) and two board-certified diagnostic radiologists (observer A, with 8 years' experience; observer B, 18 years' experience) evaluated them. The images were displayed on a commercially available diagnostic monitor in random order without clinical information or identification of the reconstruction method. Observers were asked to score visualisation of the arteries using a 4-point scale (4, completely visible; 3, partially invisible or slightly irregular appearance; 2, partially visible; 1, invisible), evaluating the main trunk of the superior mesenteric artery (SMA), its branches (right colic, middle colic, ileocolic, jejunal, and ileal arteries), the marginal arteries and vasa recta, main trunk of the celiac artery, gastroduodenal artery (GDA), and arteries of the pancreatic arcade.

Statistical analysis

We analysed statistics using SPSS software (version 25) and tested significant difference in parameters for VMI and conventional images using Mann–Whitney U test.

For subjective image analysis, we added the scores of the two observers, applied the Mann–Whitney U test to assess significant difference between their scores in each category for VMI and conventional CT images. $P < 0.05$ indicated a statistically significant difference.

To evaluate interobserver agreement, unweighted kappa coefficients were calculated for the scores of subjective analyses of conventional images and VMI images.

Results

Calculation of the modulation transfer function

Figure 2a and b shows the magnified part of the circular edge of the iodine contrast material filling the cylinder in the acrylic phantom, and Fig. 2c shows the results of MTF calculation. Higher MTFs were obtained utilising the conventional 120-kVp scan mode with both the LightSpeed VCT and Discovery CT750 HD imaging units, and the 2 scanners demonstrated no obvious difference in this mode.

Results of quantitative analysis

Table 1 shows the results of quantitative analysis. The conventional and VMI images showed no significant difference in CT attenuation of the aorta, celiac artery, SMA, and psoas major muscle. The VMI images demonstrated significantly less image noise ($p < 0.001$) and significantly higher CNRs of the aorta ($p = 0.011$) and celiac artery ($p = 0.030$) as well as a higher CNR of SMA, though the difference was not significant. In addition, the average CTDI of the VMI (13.40 ± 4.58 mGy) was significantly higher than that of the conventional scan (9.84 ± 4.31 mGy; $p =$

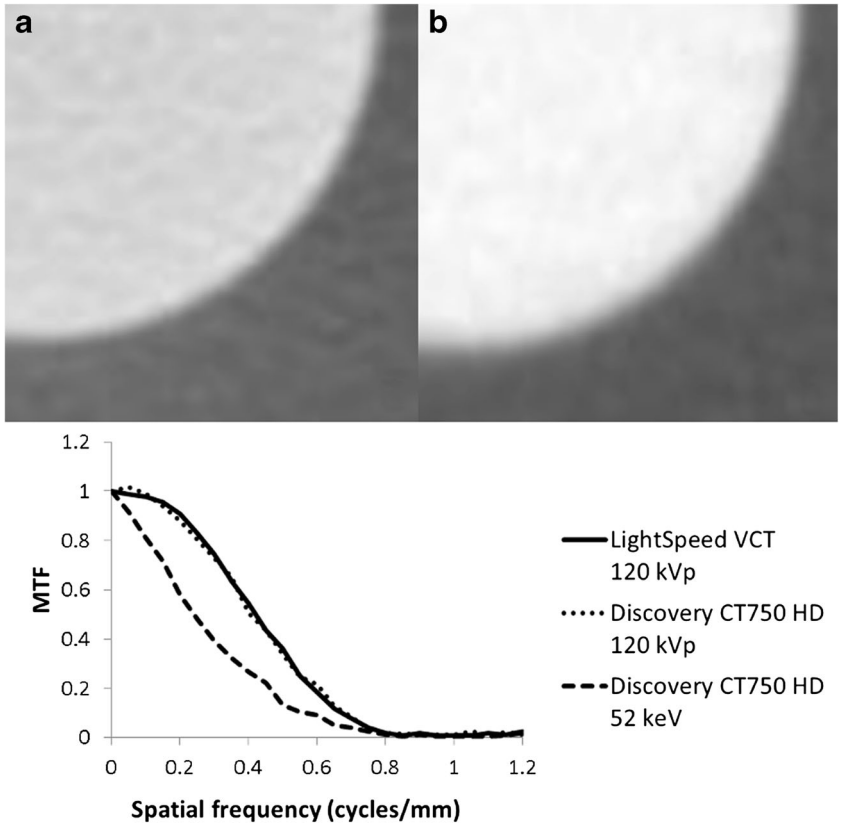

Fig. 2 Images showing the magnified part of the circular edge of the iodine contrast material obtained by (**a**) conventional 120-kVp and (**b**) virtual monochromatic imaging (VMI) at 52 keV. In the 52-keV image, the edge of circle was blurred compared with the 120-kVp image. The graph (**c**) shows the modular transfer function (MTF) for images obtained using the LightSpeed VCT and Discovery CT750 HD systems in conventional 120-kVp scanning and the Discovery CT750 HD system in 52-keV VMI

0.024). The average DLP of the VMI (920.0 ± 358.1 mGy·cm) was also significantly higher than that of the conventional scan (577.7 ± 279.6 mGy·cm; $p = 0.006$).

Results of subjective evaluation of the proximal and peripheral arteries

Table 2 and Figs. 3 and 4 show the results of evaluations by observers A and B. In most cases, both observers gave a maximum score of 4 points for visualisation of the main trunks of the celiac artery and SMA for almost all cases, and the two scan modes showed no significant difference. However, scores of the GDA, pancreatic arcade, SMA branch, marginal artery, and vasa recta were significantly higher in the conventional scan mode ($p < 0.001$). The unweighted kappa coefficients were 0.66 for the conventional images and 0.802 for the VMI. Good interobserver agreement was obtained [16]. Figs. 5 and 6 are representative images used in the subjective evaluation.

Table 1 Results of quantitative analysis

	Conventional	VMI	*p* value
Signal intensity (HU)			
Aorta	357.7 ± 50.7	371.4 ± 68.3	0.538
Celiac artery	325.8 ± 109.5	362.6 ± 67.9	0.473
SMA	354.0 ± 56.0	349.7 ± 60.8	0.715
Psoas major	57.4 ± 15.0	59.0 ± 11.4	0.801
Image noise (HU)			
Psoas major	22.5 ± 2.6	19.0 ± 2.6	< 0.001
Contrast-to-noise ratio (CNR)			
Aorta	13.5 ± 2.6	16.8 ± 4.5	0.011
Celiac artery	13.2 ± 2.7	16.3 ± 4.4	0.030
SMA	13.3 ± 2.8	15.6 ± 4.0	0.094

VMI virtual monochromatic imaging, *HU* Hounsfield units, *SMA* superior mesenteric artery

Discussion

Dual-energy CT has many clinical applications [17]. Virtual monochromatic images are produced by blending and reconstructing image data acquired at two different tube voltages. VMI permits acquisition of images at any energy level and increases the CT value of iodine at lower levels of energy that approach the K-edge energy of iodine (33.2 keV) [7]. In this way, CT attenuation in vessels can be maintained even when we reduce the dose of injected iodine in the acquisition of VMI at low energy levels [8–10]. On the other hand, image noise is known to increase as the energy level is decreased in VMI [7, 18]; so, techniques to reduce noise, such as iterative

Table 2 Mean score of subjective analysis of vessels

	Conventional Observer A	Observer B	VMI Observer A	Observer B
SMA				
Main trunk	4.00 ± 0.00	4.00 ± 0.00	4.00 ± 0.00	3.95 ± 0.22
Branch	3.86 ± 0.36	3.95 ± 0.22	3.05 ± 0.22	3.29 ± 0.46
Marginal arteries and vasa recta	2.71 ± 0.46	2.95 ± 0.22	1.95 ± 0.38	2.05 ± 0.38
Celiac artery				
Main trunk	4.00 ± 0.00	4.00 ± 0.00	4.00 ± 0.00	4.00 ± 0.00
GDA	3.52 ± 0.51	3.81 ± 0.40	3.00 ± 0.32	3.14 ± 0.36
Pancreatic arcade	2.86 ± 0.36	3.00 ± 0.32	2.10 ± 0.54	2.05 ± 0.50

VMI virtual monochromatic imaging, *SMA* superior mesenteric artery, *GDA* gastroduodenal artery

reconstruction, are commonly used in the acquisition of CT angiography with VMI using a reduced iodine dose [8–10].

In our study, CT values in the aorta, celiac artery, and SMA were maintained in VMI images despite the reduced dose of injected iodine, and the use of ASiR reduced image noise even at the low keV setting. The high CT values of vessels and reduced image noise led to higher CNRs than those obtained with conventional scanning using a full dose of injected iodine, a finding also reported in other studies [8–10].

CNR is commonly used to evaluate image quality in CT because it is easy to measure [19–21]. However, though it reflects image quality to some extent, other factors, such as spatial resolution and noise texture, also affect lesion detectability [14, 22]. It is therefore preferable to measure image quality using the method appropriate for given patient in a given situation, in other words, based on task-based analysis [22–25].

We observed no significant difference in visualisation of relatively large arteries, such as the celiac artery or SMA, but small arteries were much more difficult to detect in VMI acquired using half the conventional dose of iodine. The spatial resolution of the scan technique or reconstruction method is known to affect the visualisation of small vessels [11], and our MTF calculation suggests that spatial resolution is reduced in VMI compared with that of conventional scanning. We therefore attribute the difference in visualisation of relatively small arteries in our study to the reduced spatial resolution of VMI.

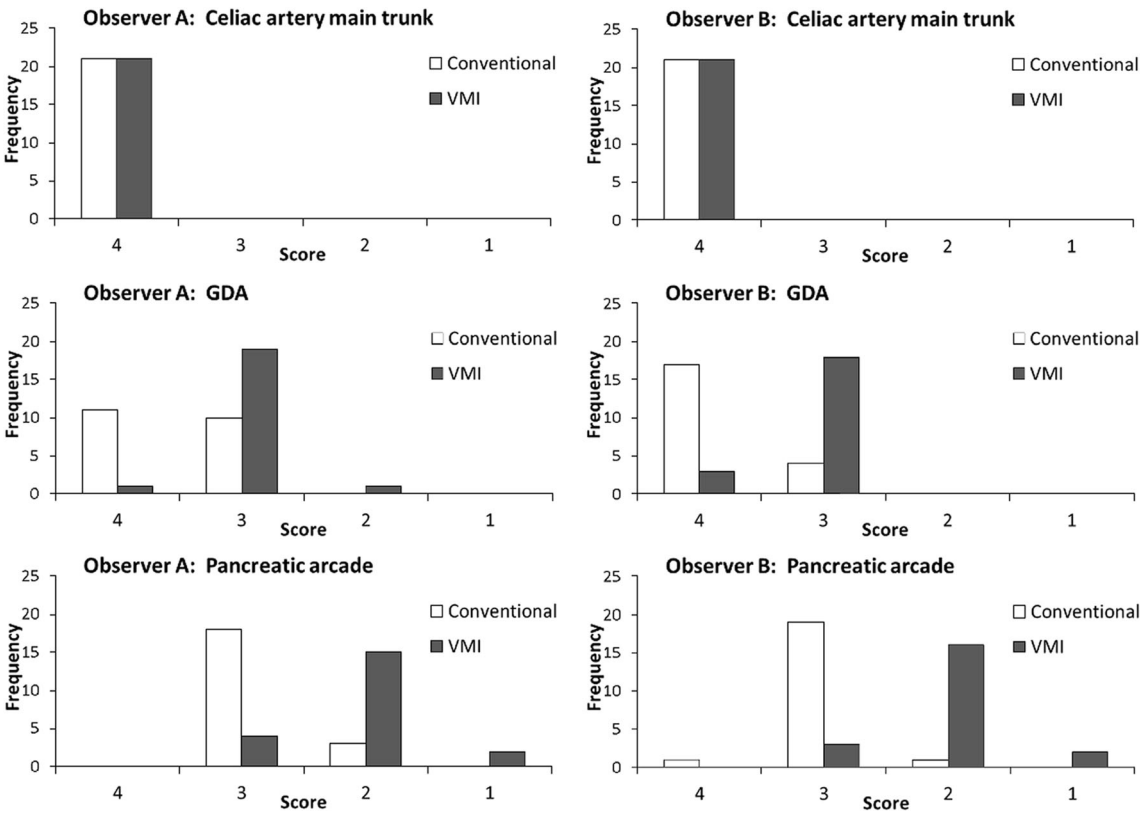

Fig. 3 Histograms show the subjective scores of observers A and B of the celiac artery branches

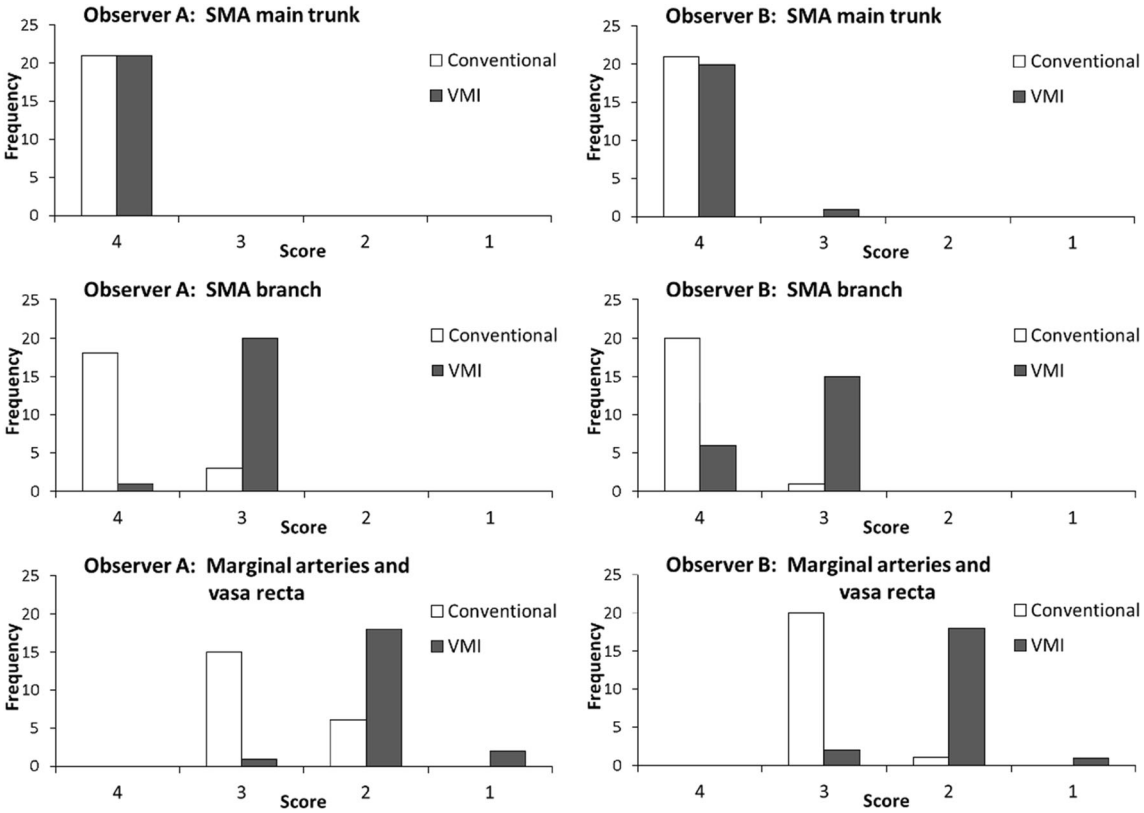

Fig. 4 Histograms showing the subjective scores of observers A and B of the branches of the superior mesenteric artery (SMA)

In patients with chronic kidney disease, the merit of reducing the injected dose of iodine to prevent contrast-induced nephropathy is tremendous. Thus, acquisition of VMI using a reduced dose of iodine is considered beneficial in the routine examination of these patients, such as for the recurrence or metastasis of disease after surgery. However, in other cases, such as for preoperative examination, we must know the precise condition of small arteries to evaluate tumour invasion or

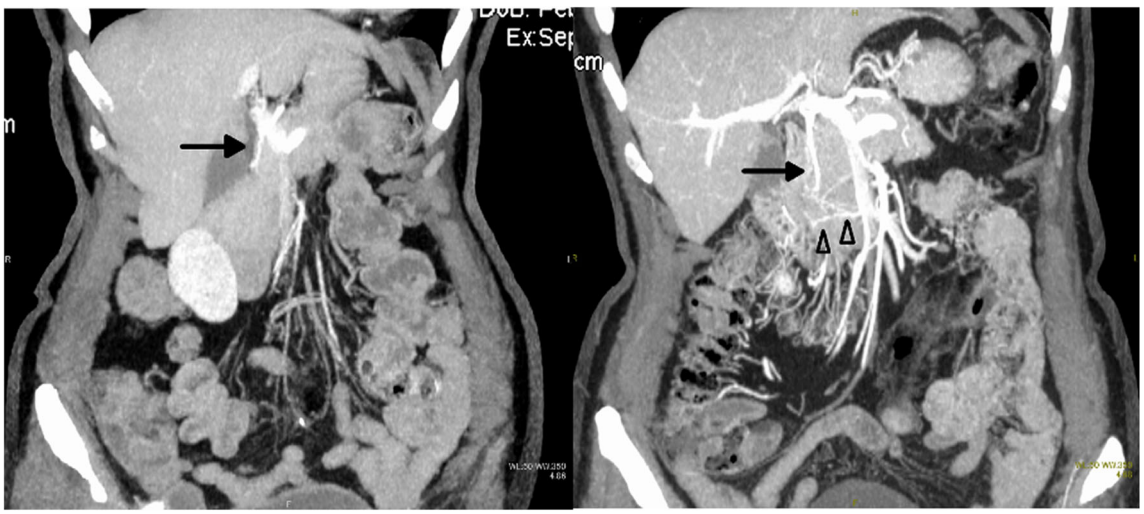

Fig. 5 Computed tomography (CT) angiography acquired utilising half-iodine virtual monochromatic imaging (VMI) (left) depicts the gastroduodenal artery (GDA) (arrow), but arteries of the pancreatic arcade are obscure. CT angiography acquired utilising full-iodine conventional CT of the same patient (right) depicts the GDA more clearly (arrow) as well as some arteries of the pancreatic arcade (arrow head). These are coronal maximum intensity projection (MIP) images (10-mm thickness, 1-mm interval). The window level was set at 50 Hounsfield units (HUs) and the window width at 350 HU

Fig. 6 Computed tomography (CT) angiography acquired utilising half-iodine virtual monochromatic imaging (VMI) (left) depicts the ileocolic artery (arrow), but the marginal arteries and vasa recta are obscure. CT angiography acquired utilising full-iodine conventional CT of the same patient (right) depicts the ileocolic artery more clearly (arrow) as well as some of the marginal arteries and vasa recta (arrow head). These are coronal maximum intensity projection (MIP) images (10-mm thickness, one-mm interval). The window level was set at 50 Hounsfield units (HU) and the window width at 350 HU

understand the vessel anatomy [1, 26]. In these cases, we have to consider the trade-off between reduction of iodine load and decreased spatial resolution.

In addition, CTDI was significantly higher in the half-iodine VMI group. One possible reason of increased radiation dose is usage of low keV level in VMI. When the dose of iodine contrast material is reduced, we have to use a low keV level to maintain contrast. Image noise is known to increase as keV level is decreased [7]; so this leads to increased radiation dose to maintain acceptable image noise. Another possible reason for increased radiation dose is unavailability of AEC in VMI. In the past study, the reduction of radiation dose by the use of AEC is reported [27]. In fast-kVp switching dual-energy CT, we cannot use AEC with the dual-energy scan mode. This possibly leads to increased radiation dose in VMI. DLP was also significantly different, but this is possibly affected by the difference of scan range between two groups.

This is a retrospective study, so the images of conventional CT angiography were obtained 1.6 years before half-iodine VMI on average. There is a possibility that the diameter of arteries became smaller because of arteriosclerotic change. Although this effect is considered to be minimal because of relatively short time span between these two scans, this is one of limitations of our study.

Another limitation of this study is that we used dual-energy CT units from a single vendor, and we believe comparison between different dual-energy systems is desirable. The decreased spatial resolution of VMI in dual-energy CT may result from misregistration between images acquired using low and high kVp settings. Misregistration is considered to be relatively mild when using a fast kVp switching technique compared to other dual-energy systems, such as the rotate-rotate technique and dual-source system, but theoretically, the dual-layer system has no misregistration [17]. The decreased spatial resolution may also be attributable to the method by which VMI images were reconstructed from two images obtained with different tube voltages. This reconstruction process is considered to be more complicated than that of conventional reconstruction and could lead to the deterioration of image quality, and different dual-energy systems offer different methods of reconstruction.

We also used only one noise reduction technique. In VMI in dual-energy CT, image noise is generally increased as the energy level selected decreases, so noise reduction is needed when the injected iodine volume is reduced and images at low keV levels are reconstructed. Some model-based iterative reconstruction algorithms are reported to improve spatial resolution as well as image noise [28, 29], and their availability for application to images acquired at low keV levels may improve the spatial resolution of VMI in dual-energy CT.

Conclusion

Large-vessel depiction and CNRs were comparable between full-iodine conventional CT and half-iodine VMI images, but VMI did not permit clear visualisation of small arteries and required a larger radiation dose.

Funding The authors state that this work has not received any funding.

Compliance with ethical standards

Guarantor The scientific guarantor of this publication is Shigeru Suzuki.

Conflict of interest The authors of this manuscript declare no relationships with any companies, whose products or services may be related to the subject matter of the article.

Statistics and biometry No complex statistical methods were necessary for this paper.

Informed consent Written informed consent was waived by the institutional review board.

Ethical approval Institutional review board approval was obtained.

Methodology
- retrospective
- performed at one institution

References

1. Hong KC, Freeny PC (1999) Pancreaticoduodenal arcades and dorsal pancreatic artery: comparison of CT angiography with three-dimensional volume rendering, maximum intensity projection, and shaded-surface display. AJR Am J Roentgenol 172:925–931
2. Winter TC 3rd, Freeny PC, Nghiem HV et al (1995) Hepatic arterial anatomy in transplantation candidates: evaluation with three-dimensional CT arteriography. Radiology 195:363–370
3. Marti M, Artigas JM, Garzón G, Alvarez-Sala R, Soto JA (2012) Acute lower intestinal bleeding: feasibility and diagnostic performance of CT angiography. Radiology 262:109–116
4. McCullough PA, Wolyn R, Rocher LL, Levin RN, O'Neill WW (1997) Acute renal failure after coronary intervention: incidence, risk factors, and relationship to mortality. Am J Med 103:368–375
5. McCullough PA, Choi JP, Feghali GA et al (2016) Contrast-induced acute kidney injury. J Am Coll Cardiol 68:1465–1473
6. Thomsen HS, Morcos SK (2003) Contrast media and the kidney: European Society of Urogenital Radiology (ESUR) guidelines. Br J Radiol 76:513–518
7. Matsumoto K, Jinzaki M, Tanami Y, Ueno A, Yamada M, Kuribayashi S (2011) Virtual monochromatic spectral imaging with fast kilovoltage switching: improved image quality as compared with that obtained with conventional 120-kVp CT. Radiology 259:257–262
8. Yuan R, Shuman WP, Earls JP et al (2012) Reduced iodine load at CT pulmonary angiography with dual-energy monochromatic imaging: comparison with standard CT pulmonary angiography–a prospective randomized trial. Radiology 262:290–297
9. Lee JW, Lee G, Lee NK et al (2016) Effectiveness of adaptive statistical iterative reconstruction for 64-slice dual-energy computed tomography pulmonary angiography in patients with a reduced iodine load: comparison with standard computed tomography pulmonary angiography. J Comput Assist Tomogr 40:777–783
10. Ma CL, Chen XX, Lei YX et al (2016) Clinical value of dual-energy spectral imaging with adaptive statistical iterative reconstruction for reducing contrast medium dose in CT portal venography: in comparison with standard 120-kVp imaging protocol. Br J Radiol 89:20151022
11. Pontone G, Bertella E, Mushtaq S et al (2014) Coronary artery disease: diagnostic accuracy of CT coronary angiography—a comparison of high and standard spatial resolution scanning. Radiology 271:688–694
12. Hinson JS, Ehmann MR, Fine DM et al (2017) Risk of acute kidney injury after intravenous contrast media administration. Ann Emerg Med 69:577–586
13. Baer RL (2003) Circular-edge spatial frequency response test. Proc SPIE 5294:71–81. Available via http://kilopixel.net/publications/EI5294-11.pdf. Accessed 5 Aug 2018
14. Richard S, Husarik DB, Yadava G, Murphy SN, Samei E (2012) Towards task-based assessment of CT performance: system and object MTF across different reconstruction algorithms. Med Phys 39:4115–4122
15. Samei E, Richard S (2015) Assessment of the dose reduction potential of a model-based iterative reconstruction algorithm using a task-based performance metrology. Med Phys 42:314–323
16. Kundel HL, Polansky M (2003) Measurement of observer agreement. Radiology 228:303–308
17. McCollough CH, Leng S, Yu L, Fletcher JG (2015) Dual- and multi-energy CT: principles, technical approaches, and clinical applications. Radiology 276:637–653
18. Sellerer T, Noël PB, Patino M et al (2018) Dual-energy CT: a phantom comparison of different platforms for abdominal imaging. Eur Radiol 28:2745–2755
19. Rose A (1948) The sensitivity performance of the human eye on an absolute scale. J Opt Soc Am 38:196–208
20. Korn A, Fenchel M, Bender B et al (2012) Iterative reconstruction in head CT: image quality of routine and low-dose protocols in comparison with standard filtered back-projection. AJNR Am J Neuroradiol 33:218–224
21. Gramer BM, Muenzel D, Leber V et al (2012) Impact of iterative reconstruction on CNR and SNR in dynamic myocardial perfusion imaging in an animal model. Eur Radiol 22:2654–2661
22. Christianson O, Chen JJ, Yang Z et al (2015) An improved index of image quality for task-based performance of CT iterative reconstruction across three commercial implementations. Radiology 275:725–734
23. Goenka AH, Herts BR, Obuchowski NA et al (2014) Effect of reduced radiation exposure and iterative reconstruction on detection of low-contrast low-attenuation lesions in an anthropomorphic liver phantom: an 18-reader study. Radiology 272:154–163
24. Jensen K, Andersen HK, Smedby Ö et al (2018) Quantitative measurements versus receiver operating characteristics and visual grading regression in CT images reconstructed with iterative reconstruction: a phantom study. Acad Radiol 25:509–518
25. Jensen K, Martinsen AC, Tingberg A, Aaløkken TM, Fosse E (2014) Comparing five different iterative reconstruction algorithms for computed tomography in an ROC study. Eur Radiol 24:2989–3002
26. Sahani D, Mehta A, Blake M, Prasad S, Harris G, Saini S (2004) Preoperative hepatic vascular evaluation with CT and MR angiography: implications for surgery. Radiographics 24:1367–1380
27. Lechel U, Becker C, Langenfeld-Jäger G, Brix G (2009) Dose reduction by automatic exposure control in multidetector computed tomography: comparison between measurement and calculation. Eur Radiol 19:1027–1034
28. Katsura M, Sato J, Akahane M, Misi Y, Sumida K, Abe O (2017) Effects of pure and hybrid iterative reconstruction algorithms on high-resolution computed tomography in the evaluation of interstitial lung disease. Eur J Radiol 93:243–251
29. Nishiyama Y, Tada K, Nishiyama Y et al (2016) Effect of the forward-projected model-based iterative reconstruction solution algorithm on image quality and radiation dose in pediatric cardiac computed tomography. Pediatr Radiol 46:1663–1670